A Secreted SPRY Domain-Containing Protein (SPRYSEC) from the Plant-Parasitic Nematode Globodera rostochiensis Interacts with a CC-NB-LRR Protein from a Susceptible Tomato

Molecular Plant-Microbe Interactions

Rehman, S.; Postma, W.J.; Tytgat, T.O.G.; Prins, J.C.P.; Qin Ling, et al

https://doi.org/10.1094/MPMI-22-3-0330

MPMI Vol. 22, No. 3, 2009, pp. 330–340. doi:10.1094/MPMI-22-3-0330. *e*-Xtra*

A Secreted SPRY Domain-Containing Protein (SPRYSEC) from the Plant-Parasitic Nematode *Globodera rostochiensis* Interacts with a CC-NB-LRR Protein from a Susceptible Tomato

Sajid Rehman,[1] Wiebe Postma,[1] Tom Tytgat,[1] Pjotr Prins,[1] Ling Qin,[1] Hein Overmars,[1] Jack Vossen,[2] Laurentiu-N. Spiridon,[3] Andrei-J. Petrescu,[3] Aska Goverse,[1] Jaap Bakker,[1] and Geert Smant[1]

[1]Laboratory of Nematology and [2]Laboratory of Phytopathology, Wageningen University, Binnenhaven 5, 6709PD Wageningen, The Netherlands; [3]Institute of Biochemistry of the Romanian Academy, Splaiul Independentei 296, 060031 Bucharest, Romania

Submitted 29 July 2008. Accepted 7 November 2008.

Esophageal gland secretions from nematodes are believed to include effectors that play important roles in plant parasitism. We have identified a novel gene family encoding secreted proteins specifically expressed in the dorsal esophageal gland of *Globodera rostochiensis* early in the parasitic cycle, and which contain the B30.2/SPRY domain. The secondary structure of these proteins, named the secreted SPRY domain-containing proteins (SPRYSEC), includes highly conserved regions folding into β-strands interspersed with loops varying in sequence and in length. Mapping sequence diversity onto a three-dimensional structure model of the SPRYSEC indicated that most of the variability is in the extended loops that shape the so-called surface A in the SPRY domains. Seven of nine amino acid sites subjected to diversifying selection in the SPRYSEC are also at this surface. In both yeast-two-hybrid screening using a library from a susceptible tomato and in an in vitro pull-down assay, one of the SPRYSEC interacted with the leucine-rich repeat (LRR) region of a novel coiled-coil nucleotide-binding LRR protein, which is highly similar to members of the SW5 resistance gene cluster. Given that the tomato cultivar used is susceptible to nematode infection, this SPRYSEC could be an evolutionary intermediate that binds to a classical immune receptor but does not yet, or no longer, triggers a resistance response. Alternatively, this SPRYSEC may bind to the immune receptor to downregulate its activity.

Parasitism of the obligate biotrophic cyst nematodes (e.g., *Globodera* and *Heterodera* spp.) essentially progresses through two stages (Hussey and Grundler 1998). In the first stage, infective juveniles hatch from eggs in the soil to invade the roots of a nearby host plant. The infective juveniles preferentially penetrate the root close to the root apex. After breaching the epidermal cell layer, they destructively migrate intracellularly within the cortex. After migration is complete, the juveniles settle and start probing host cells with their oral stylet, which marks the beginning of the second phase. One of the probed host cells is believed to respond to secretions injected into the host cell cytoplasm through the stylet of the nematode. In the hours that follow, this responsive host cell transforms into a transfer cell, on which the nematode fully depends for its development. The feeding site of the cyst nematode ultimately expands into a large syncytium generated from hundreds of cells by highly directed local cell wall degradation and subsequent protoplast fusion.

Cyst nematode esophageal gland secretions are believed to produce effectors important in plant parasitism (Davis et al. 2008). Despite significant progress in the identification of genes coding for these secretions in nematodes, little is known about the molecular targets of most of these effectors in host cells. Nor is it clear what the effects of most of the components in nematode secretions are on the constitution of the recipient host cells, and the details of the mechanisms underlying feeding site induction remain elusive. Nonetheless, it is clear that nematode effectors are crucial in host invasion, feeding structure formation and maintenance, and suppression or evasion of innate immunity in host plants.

In our approach to identify and functionally characterize effectors produced in the potato cyst nematode *Globodera rostochiensis*, we have used extensive cDNA-amplified fragment length polymorphism (AFLP) expression profiling on various developmental stages (Qin et al. 2000). The expressions of 216 transcript-derived fragments (TDF) correlated in the nematode with changes associated with parasitism. Some of these TDF derive from genes typically involved in host invasion (e.g., pectate lyase) (Kudla et al. 2007), while most of the other TDF have no homology with genes in sequence databases. One TDF (coded A18) showed similarity with human RAN-binding proteins that are capable of regulating microtubuli organization (Qin et al. 2000). Feeding-site formation involves drastic distortion of the organization of microtubuli; therefore, we have focused on the functional analysis of TDF A18. Recently, a homolog of A18 was found in a comparative transcriptome analysis of two related cyst nematode species, *G. pallida* and *G. mexicana*, which was named RAN-binding protein-1 (RBP-1) (Blanchard et al. 2005), suggesting that ho-

We dedicate this article to Dr. Ling Qin (1967–2007), who created the foundation for the discovery of the secreted SPRY domain-containing proteins with his cDNA-AFLP-based transcriptome analysis of *Globodera rostochiensis.*

Corresponding author: Geert Smant; E-mail: geert.smant@wur.nl

*The *e*-Xtra logo stands for "electronic extra" and indicates that two supplemental figures and four supplemental tables are published online. Figures 1, 4, 5, and 6 also appear in color online.

mologous genes are at least distributed within the genus *Globodera*.

In this article, we report the identification of a novel gene family with similarity to TDF A18 in *G. rostochiensis* whose members code for secretory proteins consisting of a single B30.2/SPRY domain. The SPRY domain (approximately 120 amino acids) was first identified in SPlA and in RYanodine receptors in *Dictyostelium discoideum* (Woo et al. 2006). At about the same time, the term B30.2 (approximately 170 amino acids) was coined for a domain encoded by an exon in the human class I major histocompatibility complex region. The B30.2 domain comprises a conserved C-terminal SPRY domain preceded by a more variable PRY subdomain. The SPRY domain has some structural resemblance to the immunoglobulin fold and provides an extremely versatile scaffold to facilitate intermolecular protein–protein interactions for its carrier (Rhodes et al. 2005). Therefore, we named this novel gene family the secreted SPRY domain-containing proteins (SPRYSEC) in *G. rostochiensis* and show that one of its members interacts with a coiled-coil nucleotide-binding leucine-rich repeat (CC-NB-LRR) type of disease resistance protein (Van Ooijen et al. 2008a) from the susceptible host plant tomato. Despite its interaction with a classical immune receptor protein and the discovery of diversifying selection in one its surfaces, we have found no evidence that SPRYSEC-19 activates effector-triggered immunity in host plants to date. We propose two models that could explain this phenomenon in the context of the susceptible host plant.

RESULTS

Identification of the SPRYSEC gene family.

Analysis of gene expression patterns in five distinct developmental stages of *G. rostochiensis* using cDNA-AFLP resulted in the display of 16,500 transcript-derived fragments, of which 216 were solely or predominantly expressed in potato root diffusate-exposed preparasitic second-stage juveniles (ppJ2s) and water rehydrated ppJ2s (Qin et al. 2000). The sequences of three of these TDF (A18, A41, and E19) showed significant similarity to human RAN-binding proteins (RanBPM [BAB62525], RanBP9 [AAH19886], and RanBP10 [AAI21178]). To resolve the full-length transcripts from which the TDF originated and to find homologous sequences, we first mined approximately 11,851 expressed sequence tags (EST) from *G. rostochiensis* using the TDF sequences as queries in the BLASTXN algorithm. In all, 42 matching EST were found with varying degrees of similarity to the TDF. The cDNA library clones from which the matching EST had been generated were resequenced from both ends to obtain the full insert sequences. For some of the sequences, gene-specific primers were designed to extend the sequences further at the 5′ or 3′ ends by rapid amplification of cDNA ends (RACE). Altogether, the TDF, RACE fragments, and completed library insert sequences were assembled into 35 contigs of which eight contained full-length transcripts (Supplementary Table 1).

Sequence characterization of the SPRYSEC gene family.

The eight full-length transcripts included open reading frames ranging from 208 to 274 amino acids coding for proteins with molecular masses ranging from 22.7 to 30.4 kDa (Table 1; Supplementary Table 4). For each of these eight protein sequences, an N-terminal signal peptide for secretion was predicted, whereas no trans-membrane helices were found in any of the sequences. Thus, the eight transcripts encode proteins that are likely to be secreted in or from the nematode.

A comparison of the eight protein sequences with the nonredundant protein databases resulted in significant matches with human RAN-binding proteins (GenBank accessions EAW55354 and AAI21177; *E* values < e^{-16} in BLASTP). The human RAN-binding proteins 9 and 10 are multidomain proteins of 729 and 620 amino acids, respectively, including an SPla/RYanodine receptor (SPRY) domain (pf00622), a Lissencephaly type-1-like homology motif (LisH motif; smart00667), a "C-Terminal to LisH' motif (CTLH; smart00668), and a C-terminal CT11-RanBPM domain (CRA; smart00757). The best matching putative RAN-binding protein from the free-living nematode *Caenorhabditis elegans* (CAA21656; *E* value approximately e^{-10}) has the same architecture as human RAN-binding proteins. The significant similarities between the eight predicted proteins from *G. rostochiensis* and these RAN-binding proteins are restricted to the SPRY domain of approximately 120 amino acids. A further search in the conserved domain databases using the eight protein sequences indicated that the SPRY domain is part of a larger structural domain, referred to in the literature as either B30.2, B30.2/SPRY, or PRYSPRY, and consisting of approximately 210 amino acids (IPR001870). Thus, the eight transcripts from *G. rostochiensis*, hereafter named the SPRYSEC, encode single-domain secretory proteins with strong similarity to B30.2/SPRY domains.

The SPRYSEC are expressed in the dorsal esophageal gland.

An important criterion in our strategy to identify genes involved in nematode–plant interactions is specific expression in the esophageal glands, thought to be the main source of effector proteins in plant-parasitic nematodes. To this purpose, specific antisense cDNA probes were designed within the sequences of six of the SPRYSEC (-4, -5, -8, -15, -18, and -19) for in situ hybridization microscopy on ppJ2s. The similarities of SPRYSEC-9 and SPRYSEC-16 with SPRYSEC-18 and SPRYSEC-19, respectively, were too high to allow specific probes to be made. In addition, we also designed an antisense

Table 1. Summary of the secreted SPRY domain-containing protein (SPRYSEC) family members with features of the coding region

SPRYSEC	cDNA (bp)[a]	ORF (aa)[b]	SP[c]	B30.2[d]	SPRY[e]
4	885	232	1–24	18–228	93–227
5	959	250	1–23	19–232	103–231
8	806	208	1–18	9–200	71–199
9	848	224	1–24	30–214	92–213
15	920	274	1–24	41–238	105–237
16	825	>216*	1–15	21–210	83–209
18	809	224	1–24	30–214	92–213
19	845	216	1–17	25–216	87–215

[a] Transcript length.
[b] Size of largest open reading frame (ORF) in amino acids (aa); * = start codon and a few following codons on the 5′ end of the ORF are still missing.
[c] Position of the signal peptide for secretion according to SignalP.
[d] Position of B30.2 domain (IPR001870) according to INTERPRO Scan.
[e] Position of SPRY domain (IPR003877 and PF00622) according to INTERPRO Scan.

probe within the most conserved part at the C-terminus of the SPRY domain in the SPRYSEC. All antisense probes, including the probe matching the conserved region, specifically hybridized to the dorsal esophageal gland cell (Fig. 1A through G). Also, for each of the antisense probes, we tested the corresponding sense probes, none of which resulted in a specific hybridization of tissues in whole mount nematode sections (e.g., Fig. 1H).

SPRYSEC are expressed in the early stages of the parasitic cycle of the nematode.

The SPRYSEC were identified in and cloned from ppJ2s of *G. rostochiensis* which were exposed to potato root diffusate (Qin et al. 2000). We conducted a semiquantitative reverse-transcriptase polymerase chain reaction (RT-PCR) to investigate the expression of the SPRYSEC in successive parasitic stages isolated from root tissues of nematode-infected host plants. SPRYSEC-4 and SPRYSEC-5 appeared to be upregulated in preparasitic and parasitic J2 stages only, whereas SPRYSEC-8, SPRYSEC-15, SPRYSEC-18, and SPRYSEC-19 were also upregulated in these stages but still showed some expression in later parasitic stages, albeit at lower levels than in J2s (Fig. 2). SPRYSEC-9 and SPRYSEC-16 were not sufficiently different to design gene-specific primers with amplification parameters similar to the control gene for semiquantitative RT-PCR. Reactions with uninfected root tissue and reactions without the RT enzyme were included as controls. The *cAMP-dependent protein kinase* gene from *G. rostochiensis* was used as an indicator for constitutive expression throughout the development of the nematode.

SPRYSEC are a component of stylet secretions.

We raised specific polyclonal antiserum to SPRYSEC family members to test whether the encoded proteins are a component of the stylet secretions of the nematode. The polyclonal antiserum raised to the peptides recognized three bands on Western blots (approximately 25, 32 and 37 kDa respectively) (Fig. 3A), suggesting that at least three family members were detected in the protein extracts of nematodes. Western blots of recombinantly produced SPRYSEC-15 were also probed with the antiserum to test that it indeed recognized members of the gene family (data not shown). The stylet secretions of approximately 3 million ppJ2s exposed to potato root diffusates were tested on a native dot blot for reactivity with the anti-SPRYSEC polyclonal antiserum (Fig. 3B). This antiserum detected the presence of SPRYSEC proteins in the nematode stylet secretions, whereas preimmune serum of the rabbit did not bind to the stylet secretions (Fig. 3B). A monoclonal antibody that recognizes a cellulase known to be present in the stylet secre-

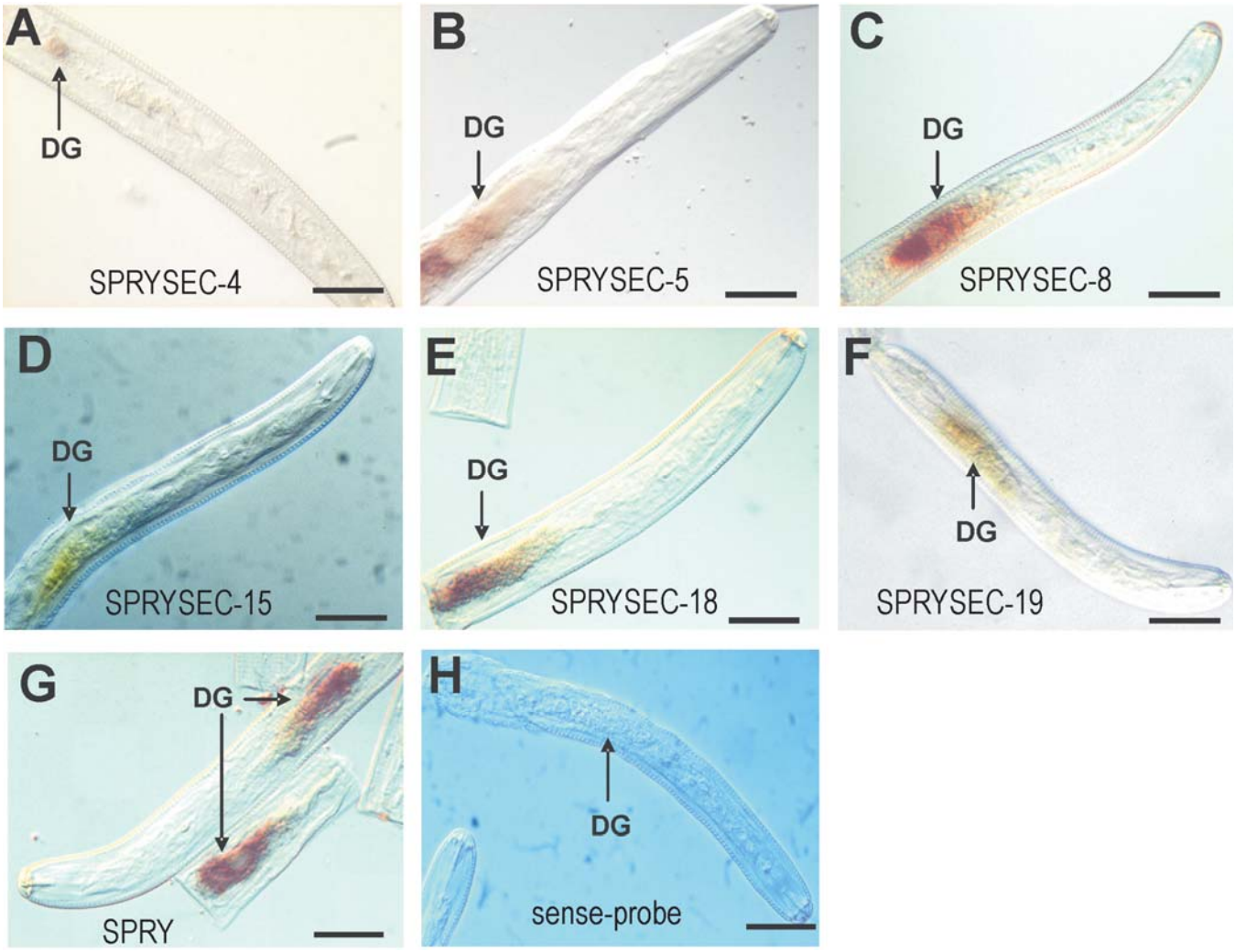

Fig. 1. A through **F,** Whole-mount in situ hybridization with antisense probes specifically designed against six secreted SPRY domain-containing proteins (SPRYSEC) in anterior sections of preparasitic second-stage juveniles of *Globodera rostochiensis* showing that each gene is expressed solely in the dorsal esophageal gland (DG). **G,** Specific hybridization of an antisense probe designed within the most conserved region of the SPRY domain in the SPRYSEC to the dorsal esophageal gland cell. **H,** Sense probes corresponding to each of the antisense probes did not show a specific hybridization.

tions of ppJ2s (Smant et al. 1997) was used as positive control and showed the expected binding pattern (Fig. 3B). Similarly, an antibody to muscle proteins of the nematodes was used to test whether contaminating proteins from nematodes, which may have been accidentally lysed during the procedure, were present in the sample and showed no binding to the collected secretions (Fig. 3B).

Diversity in the SPRYSEC gene family mainly localizes to two protein surfaces.

A protein sequence alignment of the six most related SPRYSEC family members for protein structure modeling shows an uneven distribution of the sequence similarities between family members (Fig. 4). Regions with nearly perfect sequence conservation are interspersed with regions that are highly diverged. Recently, the protein structures of three homologous B30.2/SPRY domains have been resolved: SSB-2 from *Mus musculus* with Protein Data Bank (PDB) accession 2AFJ (Masters et al. 2006), GUSTAVUS from *Drosophila melanogaster* with PDB accession 2FNJ (Woo et al. 2006), and PRYSPRY in TRIM 21 from *Homo sapiens* with PDB accession 2FBE (Grutter et al. 2006). The overall fold of these crystallized proteins is a distorted compact β-sandwich core formed by two antiparallel β sheets connected by variable loops, with two short α-helices at the N-terminus. We examined whether the sequence variability among the SPRYSEC proteins localizes to specific elements in protein folds as predicted by structure homology modeling using the resolved B30.2/SPRY structures as template. SPRYSEC-19 showed the highest level of similarity with any of the three possible templates. Also, from the three structures, GUSTAVUS showed the highest similarity with SPRYSEC-19 and the lowest level of insertions or deletions along the SPRY region and, therefore, was used as a template to model SPRYSEC-19 using remote homology modeling. The protein structure model of SPRYSEC-19 was subsequently used to build a consensus structure model of the SPRYSEC family members (Fig. 5). Most of the insertions or deletions within the SPRYSEC occur in the loops between the β-sheets that form the core of the fold of the protein. As can be readily seen, only two regions of the surface show exceptionally high variability. One highly variable area is located in the so-called surface-A region and a second region of moderate variability is located at the BC box, corresponding to the α-3 structure, following the annotation of Woo and coworkers (2006).

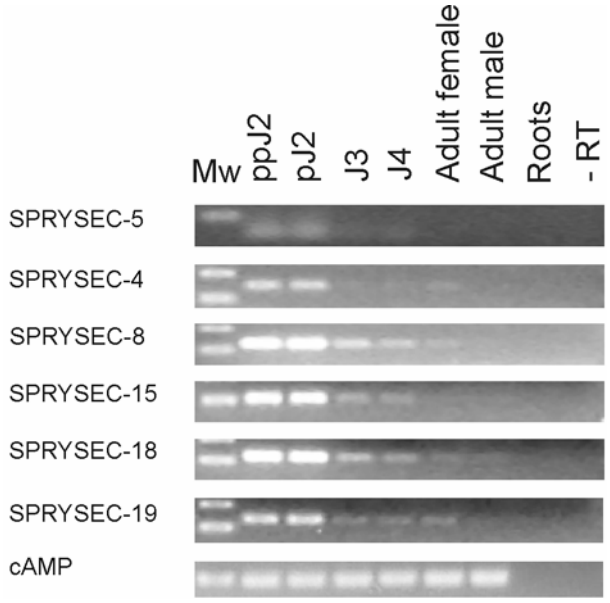

Fig. 2. Semiquantitative reverse-transcriptase polymerase chain reactions with primers specific for the secreted SPRY domain-containing proteins (SPRYSEC) on preparasitic second-stage juveniles (ppJ2) and five successive parasitic stages isolated from infected potato roots (pJ2, J3, J4, adult females, and adult males). The first lane shows the molecular weight marker, while a sample from noninfected roots (roots) and a ppJ2 sample without reverse transcriptase (–RT) were included as negative controls. The cAMP-dependent protein kinase (cAMP) from *Globodera rostochiensis* was used as an indicator for constitutive expression.

Most of the positively selected sites in the SPRYSEC localize to surface A.

Codon alignments built from cDNA and amino acid sequences of the gene family were analyzed in phylogenetic analysis by maximum likelihood (PAML) to test whether footprints of diversifying selection are detectable at specific sites in the SPRYSEC (Yang and Nielsen 2000). We statistically assessed the significance of the ω (dN/dS) > 1 per site under four different evolutionary models (M0, M3, M7, and M8). For nine sites in the alignment of the SPRY domain, we found positively selected codons, with probabilities of 0.99 and higher for ω > 1 when comparing models M3 with M0 and M8 with M7 (Fig. 4, arrow heads). Seven of nine sites under diversifying selection localize in the loops that form surface A in the structure model of the SPRYSEC.

SPRYSEC-19 interacts with an LRR domain of a CC-NB-LRR protein.

SPRYSEC-15, SPRYSEC-18, and SPRYSEC-19 were used as bait in yeast-two-hybrid (YTH) screening of a tomato root cDNA library to identify interacting host proteins. After screening of 2×10^5 independent clones, five cDNA fragments in the library activated the selection markers (AHLW + 5-bromo-4-chloro-3-indolyl-α-D-galactopyranoside [X-α-gal]) in yeast in a SPRYSEC-dependent manner for SPRYSEC-19. For SPRYSEC-15 and SPRYSEC-18, we did not find specific interactors while using these four selective nutritional markers and various other validation steps. Two of the cDNAs potentially interacting with SPRYSEC-19, named *Int-1* and *Int-2*, included an identical sequence of 894 bp. The three other clones, *Int-3*, *Int-4*,

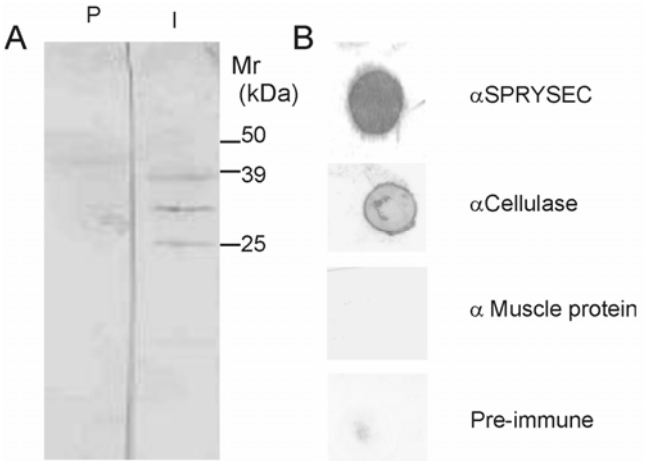

Fig. 3. A, Immunoblots of proteins extracts from homogenized preparasitic second-stage juveniles (ppJ2s) and **B,** collected stylet secretions of *Globodera rostochiensis* with a secreted SPRY domain-containing protein (SPRYSEC)-specific polyclonal antiserum. **A,** Western blot of a nematode homogenate probed with anti-SPRYSEC polyclonal antiserum raised in a rabbit (I) and pre-immune serum from the same rabbit (P). **B,** Dot blot of collected stylet secretions from 3 million ppJ2s exposed to potato root diffusate probed with anti-SPRYSEC antiserum, anticellulase antibody MGR048, antimuscle antibody MGR007, and a preimmune serum from rabbits.

and *Int-5*, harbored identical cDNAs coding for a protein sequence with weak similarity to open reading frames in *Arabidopsis thaliana* and *Oryza sativa*, which were not further investigated. The interaction between SPRYSEC-19 and *Int-1* and *Int-2* could be abolished by disrupting the open reading frame (Fig. 6A). The interaction between SPRYSEC-19 and *Int-1* and *Int-2* was further validated in vivo by yeast mating (data not shown) and by reciprocal swapping of the BD and the AD plasmids for the bait and preys (Fig. 6A). Furthermore, SPRYSEC-19 in AD conformation (SPRYSEC-19-AD) did not show autoactivation of auxotrophic yeast strain (AH109) on selective media (without the amino acids AHTL) when co-transformed either with empty vector (BD-E) or with BD-lamin. Similarly, *Int-1* and *Int-2* did not show autoactivation when co-transformed either with empty vector (BD-E) or with BD-lamin. Thus, in yeast, the interaction between SPRYSEC-19 and *Int-1* and *Int-2* was specific.

The AD-plasmid carrying *Int-1* and *Int*-2 was rescued from yeast for sequencing of the insert. BLASTX analysis of the insert sequences on the nonredundant database revealed highly significant similarity with the so-called LRR region of several *Tospovirus* (*Tomato spotted wilt virus*) resistance gene homologues from the SW5 resistance gene cluster (AAG31013 through 17), a nematode resistance protein Mi-1.2 (AAC32252), a *Pseudomonas syringae* resistance gene PRF (AAC49408), and the *G. rostochiensis* resistance genes Hero (CAD29729) and Gpa-2 (AAF0403). Because *Int-1* and *Int-2* was highly similar to members of the SW5 cluster from tomato (i.e., SW5A through E), we named it LRR-SW5-F.

LRR-SW5-F matched the C-terminal 194 amino acids of the LRR domain in members of the SW5 resistance gene cluster in tomato. The members of the SW5 cluster belong to the CC-NB-LRR class of resistance proteins (Spassova et al. 2001) and, therefore, it was likely that LRR-SW5-F represented only the C-terminus of a larger protein. In order to clone the missing 5′ end of LRR-SW5-F, a degenerate primer (SW5CD) (Supplementary Table 2) designed at the 5′ end of the members of the SW5 cluster and a gene-specific reverse primer (Int-1/2-R) designed within the 3′ untranslated region of LRR-SW5-F were used to PCR amplify a product of 3,992 bp from tomato cDNA. This transcript, named SW5-F, encodes a protein of 1,275 amino acids with a predicted molecular mass of 147 kDa (Supplementary Fig. 1). The 3′ untranslated region consists of 282 bp and a putative polyadenylation signal is located 251 nucleotides downstream of the stop codon. BLASTP searches in a nonredundant-protein database using the full SW5-F sequence as query again revealed an extremely high similarity (*E* values close to 0) with *Tospovirus* resistance gene homologues from the SW5 cluster in tomato (Supplementary Table 3).

The architecture of SW5-F displays the typical features of the CC, NB (NB-ARC), and LRR family of resistance genes (Fig. 6C). SW5-F is of approximately the same size as Mi-1.2, SW5-A, SW5-B, SW-5C, SW5-D, and SW5E, while PRF includes a long N-terminal extension of approximately 300 amino acids. The N-terminal region of SW5-F (amino acids 1 to 407) showed weak homology with the Solanaceae Domain (SD) (Mucyn et al. 2006). Next to the SD of SW5-F (amino acids 435 to 449), a CC is predicted by the COILS program (window 14, with probability of 0.925 and higher), which was also reported for SW5A and SW5B (Spassova et al. 2001). The central NB-ARC1-ARC2 domain contains all the conserved motifs, including the hhGRExE, RNBS, Walker A and B, GLPL, and MHD (VHD in SW5F) motifs as reported for all other disease resistance genes of the NB-LRR family (Van Ooijen et al. 2008b). In addition, the C-terminal region of

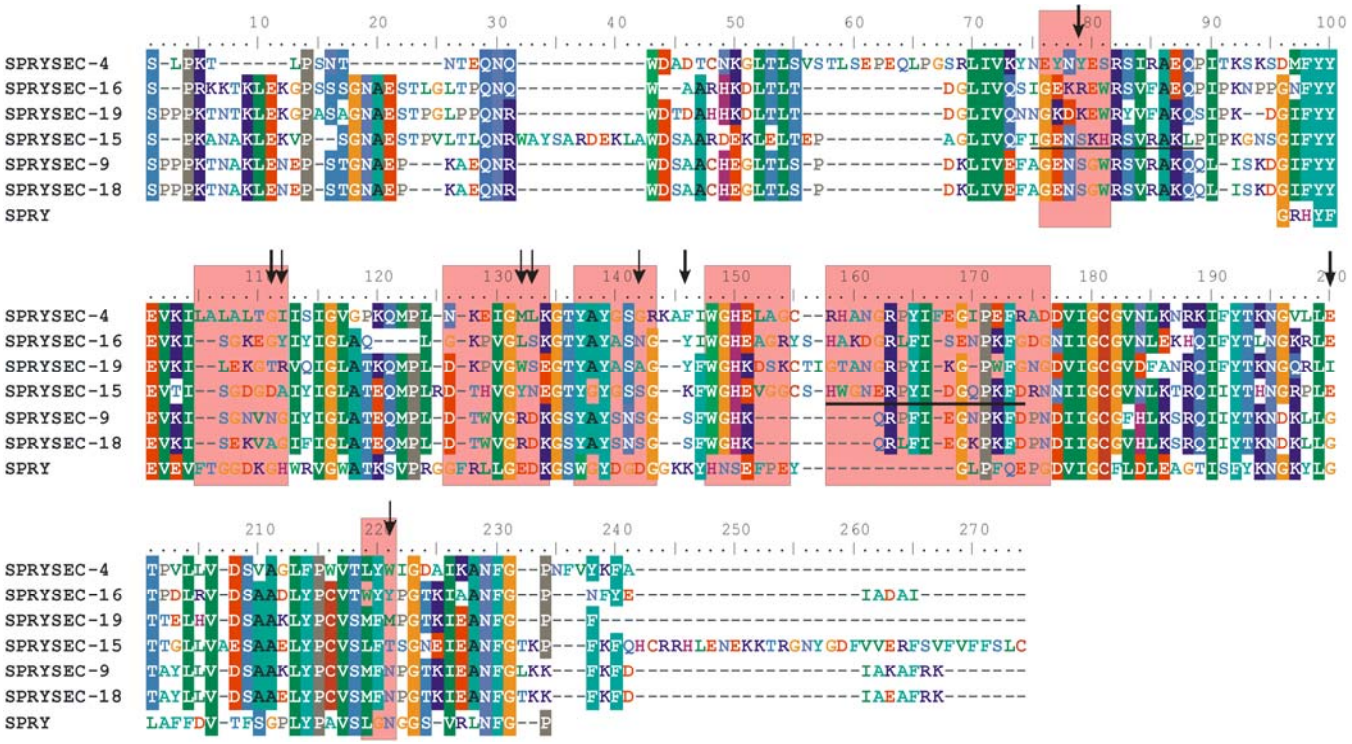

Fig. 4. Multiple protein sequence alignment of the secreted SPRY domain-containing proteins (SPRYSEC) most similar to SPRYSEC-19 and the consensus sequence of the SPRY domains in the PFAM accession (PF00622) made for the three-dimensional structure modeling. The residues shaded in pink indicate the conservation level in a column is 80% or higher. The residues are color coded according to the BLOSUM62 table. The boxed residues indicate the extended loops in the protein structure that are part of the surface A in SPRY domains (Woo et al. 2006). The nine arrowheads indicate positions in the aligned sequences with a probability higher than 0.99 to have been subjected to diversifying selection. Underlined residues are the sequences of the synthetic peptides used to raise the polyclonal antiserum to the SPRYSEC. The signal peptides were removed prior to aligning the sequences.

SW5-F encodes an LRR, very similar in size to that of SW5-A, SW5-B, SW5-C, SW5-D, SW5-E, Mi-1.2, and PRF. SW5-F is predicted to have 13 repeats in the LRR domain, largely following the consensus sequence xxLxLxx (starting from amino acid position 939). In conclusion, SW5F, therefore, has the same CC-NB-LRR architecture as classical receptors of the plant's innate immune system.

A pull-down assay was used to confirm the interaction between SPRYSEC-19 and the LRR region of SW5-F in vitro (Fig. 6B; Supplementary Fig. 2). For this purpose, SPRYSEC-19 was expressed as an N-terminal gluthathione-S-transferase fusion protein (GST-SPRYSEC-19, approximately 48 kDa) immobilized on sepharose beads. LRR-SW5-F fused to thioredoxin (THIO-LRR-SW5-F, approximately 40 kDa) was incubated with either GST-SPRYSEC-19 immobilized to the beads or GST immobilized to the beads alone (approximately 35 kDa). After extensive washing, bound proteins were resolved by sodium dodecyl sulfate polyacrylamide gel electrophoresis (SDS-PAGE) and Western blotting with antisera recognizing either GST or THIO (Nguyen and Goodrich 2006). The THIO-LRR-SW5-F bound specifically to GST-SPRYSEC but not to GST alone. Similarly, thioredoxin alone (THIO, 19.5 kDa) did not bind to GST-SPRYSEC-19 on sepharose beads or to sepharose beads alone.

DISCUSSION

The plant-parasitic nematode *G. rostochiensis* delivers the products of its parasitism genes (effectors) directly into host tissues through an oral stylet. These effectors are crucial for host invasion, feeding, and modulation of the host defense responses. Here, we present a novel gene family in *G. rostochiensis* coding for a B30.2/SPRY domain in the nematode's stylet secretions. The SPRY is an extremely versatile domain, which so far has been found in 53 different architectures with a variety of other domains (see PFAM accession PF00622) (Ponting et al. 1997). SPRYSEC consist solely of a single B30.2/SPRY domain and a signal peptide for secretion. Other proteins with exactly the same architecture are found in the venom glands of venomous snakes and lizards. This protein family, named the *vespryn* (the name derives from venom PRY-SPRY domain containing proteins with a signal peptide), includes four members so far: ohanin/pro-ohanin (Pung et al. 2006), lizard venom (Fry et al. 2006), thaicobrin (Junqueira-

Fig. 5. Consensus model of three-dimensional protein structure based on the sequences of secreted SPRY domain-containing protein (SPRYSEC)-4, SPRYSEC-5, SPRYSEC-8, SPRYSEC-9, SPRYSEC-15, SPRYSEC-16, SPRYSEC-18, and SPRYSEC-19 using the Potato Data Bank accession 2FNJ (GUSTAVUS) as template. The degree of sequence variation is mapped onto the protein structure as a color-coded heat map ranging from high similarity in blue to low similarity in red. Surface A of the SPRY domains is circled, and the C-terminal region with structural similarity to the BC box is boxed (Woo et al. 2006).

de-Azevedo et al. 2006), and ohanin-like protein (Li et al. 2004). Another group of secreted B30.2/SPRY proteins are the stonustoxins from the stonefish (*Synanceja horrida*) (Ghadessy et al. 1996) and the neoverrucotoxins from the stonefish (*S. verrocusa*) (Ueda et al. 2006). These stonefish toxins form multimeric complexes of large subunits (70 to 85 kDa) with the B30.2/SPRY domain at the C-terminus of each subunit. Despite having similar domain architectures, none of the proteins mentioned above have significant similarity to primary amino acid sequences of the SPRYSEC. Therefore, the use of the B30.2/SPRY domain in plant–microbe interactions seems to be an evolutionary innovation in nematodes.

The best matching sequences in the database for the SPRYSEC were the SPRY domains of metazoan RAN-binding proteins. However, the SPRYSEC are much smaller than RAN-binding proteins (approximately 27 versus 65 to 70 kDa) and lack the typical LisH and the CTLH domains (Murrin and Talbot 2007). The physical interaction between *ran* and RANBPM is likely mediated through its SPRY domain. Therefore, it could be argued that the SPRYSEC still exert their activity in a manner still similar to that of RAN-binding proteins. In a yeast-two-hybrid analysis with two *ran* genes from tomato and SPRYSEC-19, we have not found a physical interaction (data not shown). Ectopically expressed metazoan RanBPM interferes with the dynamic stability of microtubuli, which leads to uncoordinated aster formation in the recipient cells (Nakamura et al. 1998). Overexpression of SPRYSEC-15 and SPRYSEC-19 in a transgenic tobacco cell line with microtubule-associated protein MAP4 fused to green fluorescent protein did not show abnormal microtubule organization (data not shown). Therefore, we conclude that the B30.2/SPRY domain in SPRYSEC and in RAN-binding proteins in nematodes may have a common evolutionary history. However, both the protein architecture of the SPRYSEC, which is fundamentally different from the multidomain architecture of RAN-binding proteins, and the experimental data presented here suggest that they have acquired different functions.

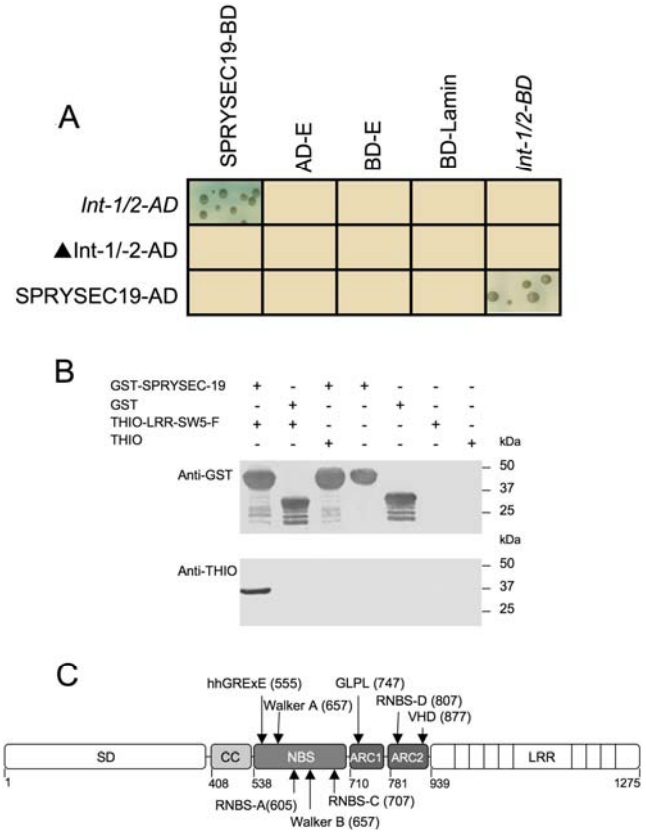

Fig. 6. A, INT1/2 fused to the activator domain of GAL4 (Int1/2-AD) specifically interacts with secreted SPRY domain-containing protein (SPRYSEC)-19 fused to the DNA binding domain of GAL4 (SPRYSEC-19-BD) in a yeast-two hybrid analysis. The reciprocal constructs with leucine-rich repeat (LRR)-SW5F fused to BD (Int1/2-BD) and SPRYSEC-19 fused to AD (SPRYSEC-19-AD) also show interaction. The LRR-SW5F and the SPRYSEC-19 constructs do not lead to autoactivation of GAL4 yeast when combined with empty vector controls (AD-E and BD-E), and with lamin fused to BD of GAL4. Disrupting the open reading frame of LRR-SW5F (ΔInt1/2) also eliminates the interaction with SPRYSEC-19. **B,** GST pull-down assays of recombinant LRR-SW5F fused to thioredoxin (THIO-LRR-SW5F) by the SPRYSEC-19 fused to GST and immobilized on sepharose beads (GST-SPRYSE-19). A pull-down of THIO-LRR-SW5F failed with GST immobilized alone on sepharose beads (GST), and of thioredoxin alone (THIO) with GST-SPRYSEC-19 immobilized on sepharose beads. The Western blot probed with antiserum to GST (A) shows the presence of GST-SPRYSEC-19 or GST alone on the beads, whereas the anti-THIO serum shows the specific binding of THIO-LRR-SW5F to beads carrying GST-SPRYSEC-19. **C,** Architecture of SW5F, including the Solanaceae Domain (SD), coiled-coil (CC), nucleotide-binding site (NBS), ARC1, ARC2, and LRR domains, matches that of Solanaceous CC-NB-LRR immune receptors. The numbers indicate the positions of the various motifs.

In addition to its binding to *ran*, the SPRY domain in RAN-binding proteins has been shown to interact with a variety of other proteins mostly involved in signaling, including several receptor protein-tyrosine kinases. For example, the SPRY domain of RanBP9 interacts with MET, a receptor protein kinase for the hepatocyte growth factor, which is a multifunctional cytokine controlling cell growth, morphogenesis, and motility (Wang et al. 2002). RanBPM has also been shown to interact through its SPRY domain with intracellular domain of neurotrophin receptor Trk (Yuan et al. 2006). Similarly, the SPRY domain of RanBPM mediates the interaction between RanBPM and human dectin-1 transmembrane receptor isoform hDectin-1E (Xie et al. 2006). It has also been demonstrated that RanBPM interacts with integrin LFA-1 and is phosphorylated within the SPRY domain at residue Thr320 both constitutively and in response to stress by p58 kinase (Denti et al. 2004). Evidently, the SPRY domain in RAN-binding proteins is capable of interacting with a diverse range of receptor-like proteins, which mostly seems to lead to modulation of downstream signal-transduction pathways.

Typically, alignments of SPRY domains show conserved blocks interspersed with highly variable stretches of varying length and sequence in the loops at the surface of the protein (Rhodes et al. 2005). We found that most of the amino acid sites under diversifying selection in the SPRYSEC are also in these loops, suggesting that this hypervariable surface interacts with host targets. It should be noted that, because of a lack of sufficient alignment between members of the SPRYSEC gene family within the loops, which impedes further analysis in PAML in these regions, the number of sites under diversifying selection suggested here may even be an underestimate. Seto and co-workers (1999) noted that the core structure of the SPRY domain is reminiscent of the classical immunoglobulin fold of a stable scaffold with hypervariable complementarity-determining regions, which are located in the extended loops at one side of the β-sandwich. More recent work suggests, however, that the actual topology of the B30.2/SPRY domain represents a novel fold distinct from the immunoglobulin fold (Masters et al. 2006). Nonetheless, the concept of a stable scaffold with hypervariable complementarity-determining regions located in the extended loops at one side of the β-sandwich seems applicable to the SPRY domain in SPRYSEC as well. The wide range of binding specificities in immunoglobulins is brought about by variations in length and in amino acid sequence in the hypervariable loops (Wilson and Stanfield

1993). A preliminary study of the genetic and allelic variation in SPRYSEC in *G. rostochiensis* suggests that this gene family includes many more members (>50) with sequence and length variations primarily in the extended loops (T. Tytgat, *personal communication*). Therefore, we conclude that the SPRY domain is probably used in SPRYSEC in *G. rostochiensis* as a versatile scaffold with a hypervariable surface capable of targeting many different host proteins. Preliminary searches in the dEST database and in newly published genomes indicate that SPRYSEC homologs also constitute large gene families in *G. pallida, Heterodera schachtii*, and *H. glycines*. In contrast, the genome of the root-knot nematode *Meloidogyne incognita* does not include SPRYSEC homologs (Abad et al. 2008), suggesting that the distribution of the SPRYSEC may be specific for cyst nematodes.

We used a combination of yeast-two-hybrid analysis and in vitro GST pull-down assays to demonstrate a specific physical interaction of the nematode effector SPRYSEC-19 with the LRR region of the *Tospovirus* resistance gene homolog SW5-F from tomato. The CC-NB-LRR architecture of SW5-F is typical of the CC-NB-LRR class of disease resistance genes. Furthermore, SW5F is highly similar to members of the SW5 disease resistance cluster in tomato (*E* value of 0 with 69 to 83% identity and 79 to 87% similarity over 1,275 amino acids), suggesting that it could be a functional resistance gene. In the gene-for-gene model for disease recognition specificity, resistance (R) proteins activate a resistance response, often a hypersensitive response, only when they detect the presence of specific pathogen effectors (Jones and Dangl 2006). Detection can be either direct or indirect, via changes in another guarded host protein. The tomato cultivar harboring the SW5-F gene is susceptible to potato cyst nematodes expressing SPRYSEC-19. Nonetheless, we tested whether SPRYSEC-19 activates an SW5-F-dependent hypersensitive response in plants. We found that transient coexpression of SW5-F and its interacting nematode effector SPRYSEC-19 does not evoke a hypersensitive response in *Nicotiana benthamiana* (data not shown). Consequently, we have no evidence that the interaction between SW5-F and SPRYSEC-19 conditions resistance to the nematodes in tomato.

Thus, our findings lead us to two possible models for the role of SPRYSEC-19 and SW5F in nematode–plant interactions, which are not mutually exclusive. In the first model, the physical interaction between SPRYSEC-19 and SW5F is an evolutionary intermediate. There is evident binding between a nematode protein and a host plant protein, but this does not lead to the activation of disease resistance signaling (anymore). Other *R* gene homologs of SW5F may exist in various (resistant) host plants that both bind SPRYSEC-19 and elicit a resistance response following the interaction. Alternatively, homologs of SPRYSEC-19 that also bind to SW5F and do elicit a resistance response may exist in other (avirulent) *G. rostochiensis* populations. Although the outcome of our coexpression experiment in *N. benthamiana* does not point in that direction, in principle, SPRYSEC-19 could be able to trigger an immune response via its interaction with SW5F but other co-secreted nematode effectors may suppress this response, rendering the plant fully susceptible to infection (Jones and Dangl 2006).

In our second model, SPRYSEC-19 binds to SW5-F to promote the virulence of the nematode by modulating host defense responses. Interestingly, a parallel may be found in the protein that was used as modeling template for the SPRYECs, the SOCS-box-containing protein GUSTAVUS (Woo et al. 2006). GUSTAVUS binds VASA via its SPRY domain and the heterodimer elongin B and C through its BC box. Elongin BC connects SOCS-box-containing proteins to the so-called elongin C-cullin-SOCS-box (ECS) type of E3 ubiquitin ligase. SOCS-containing proteins such as GUSTAVUS may target proteins bound to the SPRY domain to the proteosomal degradation pathway and, thereby, regulate their turnover rate (Kile et al. 2002). At the C-terminus of the protein structure model of the SPRYSEC is an α-helical structure that is reminiscent of the BC box in GUSTAVUS. Therefore, we hypothesize that some of the SPRYSEC family members may act as adapters to confer diverse recognition specificities to E3 ubiquitin ligase complexes of the host. Thus, the SPRY domain in SPRYSEC could provide a hypervariable binding surface within a stable scaffold structure, which may be tuned to interact with a variety of host proteins. Modifying their rate of turnover may regulate the molecular targets of the SPRYSEC in host cells; for instance, components in the innate immune system in plants. Further research is required to identify more molecular targets of the SPRYSEC in host cells and to study the possible involvement of the host's ubiquitination machinery in SPRYSEC-mediated regulation of these targets.

MATERIALS AND METHODS

Nematodes.

Dried cysts of *G. rostochiensis* pathotype Ro1 Mierenbos were soaked on a 100-μm sieve in potato root diffusate to collect hatched ppJ2s (De Boer et al. 1992). Freshly hatched ppJ2s in suspension were mixed with an equal volume of 70% (wt/vol) sucrose in a centrifuge tube and covered with a layer of sterile tap water. Following centrifugation for 5 min at 1,000 × *g*, juveniles were collected from the sucrose–water interface using a Pasteur pipette and washed three times with sterile tap water. Parasitic stages were isolated from roots of potato cv. Bintje at 13, 19, 23, 27, and 34 days post inoculation to yield samples of second-, third-, and fourth-stage juveniles and adult males and females, respectively. For this purpose, infected roots were cut into small pieces with a blender and nematodes were separated from root debris on sieves with a mesh of 250, 175, 100, 22, and 10 μm. The isolated nematodes were either used for experiments directly or stored at –80°C until further use.

Cloning, sequencing, and analysis of SPRYSEC.

The DNA sequences of TDF were used to mine the 10,000 EST from preparasitic and parasitic J2s of *G. rostochiensis*. The library clones from which the EST were subsequently sequenced used the T7 and the SP6 primer site of the pCDNAII library plasmid (Baseclear, Leiden, the Netherlands). The sequences were assembled into contigs and checked for likely complete open reading frames as well as the presence of a polyA-tail. For contigs that were suspected to include partial reading frames, primers were designed to amplify flanking regions up- and downstream with the RACE (Invitrogen, San Diego, CA, U.S.A.). Contig assembly was done using Contig Express of the VectorNTI software package (Invitrogen). The assembly criterion was set at 100% identity in a minimal overlap of 100 nucleotides.

Semiquantitative RT-PCR.

Messenger RNA was extracted from five developmental stages of *G. rostochiensis* pathotype Ro1-Mierenbos essentially as described previously (Qin et al. 2000). RT-PCR was performed using Superscript III following the manufacturer's protocols (Invitrogen) (Kudla et al. 2007). Total RNA isolated with TRIzol (Invitrogen) was treated with Turbo DNA-free (Ambion, Austin, TX, U.S.A.) to degrade contaminating genomic DNA. Messenger RNA was subsequently isolated from total RNA samples using the Dynabead mRNA purification

system (Invitrogen). First-strand cDNA synthesis was primed with a mix of random hexamer and oligo-dT primers in a reaction containing 0.5 mM dNTPs, 0.1 units of RNase-out, and 10 units of Superscript III that was incubated for 60 min at 50°C and 15 min at 70°C. Prior to the PCR, the samples were incubated with two units of RNase-H for 20 min at 37°C. Fragments of SPRYSEC were PCR amplified for 26 cycles with gene primers, whereas specific forward and reverse primers were used to amplify a 91-bp fragment of the constitutively expressed cAMP-dependent protein kinase (*Gr-cAMP*; GenBank accession number BM343563). We included reactions without RT to test for possible amplification of the target genes from contaminating genomic DNA. A sample made from noninfected roots was used to check for nonspecific amplification from host plant tissues.

In situ hybridization microscopy.

DNA probes were amplified from the SPRYSEC by using specific oligonucleotide primers and digoxigen-11-dUTP. ppJ2s were fixed overnight in 2% paraformaldehyde, cut into sections, and permeabilized as described (De Boer et al. 1998; Smant et al. 1998). Fixed sections were then incubated at 50°C with sense or antisense DNA probes followed by digestion with RNAse A and stringency washes. The hybridized DNA probe was detected using an antidigoxigenin antibody and alkaline phosphatase staining (Genius kid, Boehringer Mannheim, Mannheim, Germany). Stained J2s were examined with differential interference contrast microscopy (Leica, Deerfield, IL, U.S.A.).

Antiserum and immunodetection.

Polyclonal antiserum was raised to synthetic peptides designed from the SPRYSEC gene family members (Eurogentec, Ghent, Belgium). For this purpose, two antigenic peptides (IGENSKHRSVRAKLPC [present in SPRYSEC-9, SPRYSEC-15, and SPRYSEC-18] and HWGNERPYIDGQPKFD [present in all SPRYSEC]) were used for the immunization of rabbits.

Western blots of homogenates of ppJ2s were performed as described by (De Boer et al. 1996). Proteins were separated on 12.5% denaturing polyacrylamide gels by SDS-PAGE and subsequently transferred onto 0.2-µm nitrocellulose membrane (Schleicher and Schuell, Keene, NH, U.S.A.) using a semidry blotter with dry blot buffer (48 mM Tris, 150 mM Glycine, 10% methanol, pH 8.3). The blots were probed with different primary antibodies, including anti-GST (Amersham, Little Chalfont, U.K.), anti-thioredoxin (Invitrogen), and anti-SPRYSEC, and detected with alkaline-phosphatase-conjugated rabbit anti-goat, rabbit anti-chicken immunoglobulin Y, and rat anti-mouse (Jackson Immunoresearch Laboratories, Inc., West Grove, PA, U.S.A.), respectively. The blots were developed in substrate buffer supplemented with nitroblue-tetrazolium and 5-bromo-4-chloro-3-indolylphosphate (Sambrook et al. 1989).

Dot blots of collected stylet secretions were made as was described previously (Smant et al. 1997). The dot blots were probes with anti-SPRYSEC serum, anti-cellulase monoclonal antibody MGR048 (Smant et al. 1998), and a monoclonal antibody to nematode muscle protein MGR007 (De Boer et al. 1996).

PAML.

The six sequences most similar to SPRYSEC19 were tested for positive selection, including SPRYSEC-4, SPRYSEC-9, SPRYSEC-15, SPRYSEC-16, and SPRYSEC-18. The ratio ω was estimated with the CODEML program of PAML (Yang 2007). Two models of fitting codon substitution were used to calculate likelihood ratio statistics (LR), twice the log-likelihood between models is compared with the value of a χ^2 distribution with branches-1 degrees of freedom. Model M7 (β-distributed variable selection pressure) has an ω for each site drawn from a β distribution with parameters p and q. Model M8 (β plus $\omega > 1$) uses the M7 recipe for a fraction p_0 of the sites and assigns another ω to the remaining fraction. When M8 fits the data significantly better than M7 and the ω ratio estimated under model M8 is greater than 1, we assume evidence of positive selection. To check whether it is significantly greater than 1, the log-likelihood value in M8 is recalculated fixing ω to be 1 and compared with the change in likelihood with a χ^2 distribution with 1 degree of freedom. Likewise, the less complicated models M0 (uniform selective pressure among sites) with M3 (variable selective pressure among sites) were calculated and the results were found to give less conservative estimates than M7/M8. The amino acid sequence alignment was generated in ClustalX (v1.83) (Chenna et al. 2003), and pal2nal (v11) (Suyama et al. 2006) was used to relate the sequences back to a nucleotide alignment.

Three-dimensional structure modeling.

Fold recognition analysis of the SPRYSEC was performed with Phyre (Bennett-Lovsey et al. 2008). The best three hits were all SPRY-domain-containing proteins, including GUSTAVUS from *D. melanogaster* (PDB accession 2FNJ with *E* value of 2.6e-14 and 100% precision), SSB-2 from *Mus musculus* (PDB accession 2AFJ with *E* value of 1.3e-13 and 100% precision), and PRYSPRY of TRIM21 from *Homo sapiens* (PDB accession 2FBE with *E* value of 1.3e-05 and 95% precision). Further confirmation of these hits was achieved by comparing them with the HMM profiles in PFAM accession PF00622 and SMART accession SM00499. At the level of the primary sequence, the best match was found between SPRYSEC-19 and GUSTAVUS (12% identity and 37% similarity). In spite of these low similarities, remote homology modeling was reliably possible due to the good match between the secondary structures of template and target, the accessibility, and the contact propensity profiles. This data was collectively incorporated into the refined alignment and the profilings were subsequently performed with the best methods ranked by CASP4 (HNN, PROG, Jpred, and GOR-IV). Homology modeling was performed with Insight II software package (Accelrys, Cambridge, UK). The homology module in Insight II was used for coordinate transfer and loop generation. Local simulated annealing and energy minimization during modeling steps were performed via the Discovery Studio module with Class II Force Field using CVFF force field. The approach was to transfer the coordinates along the stretches that form the β-sandwich core and to generate ab initio the loops between the β structures. To map the variability within the SPRYSEC, we also built a consensus model using as target the consensus sequence of the five most similar SPRYSEC. The variability at a given position was defined as the average of the Blosum62 substitution matrix values between every sequence and the consensus.

$$\sum_i \frac{M(S_{ij}, C_j)}{i}$$

where S_i = sequence i, C = consensus sequence, and j = position.

Yeast two-hybrid screening.

The prey tomato root cDNA library used in present study has been described earlier (De La Fuente Van Bentem et al. 2005). The library consisted of 2 million independent clones with an average insert size of 1.1 kb. The MATCHMAKER Two-hybrid System 3 (Invitrogen) was used to construct all the bait and prey constructs used this study. For SPRYSEC-19 bait construction, the coding region of SPRYSEC-19 was amplified

with primers YA18-F and YA18R by PCR. The amplification products were cloned in frame with Gal4 DNA-binding domain of vector pGBKT7 (Invitrogen) using *Nde*I and *Bam*HI restriction sites. For the construction of ▲Int-1/2-AD, the reading frame was disturbed by recloning the Int-1/2 insert from pACT2 into pGADKT7 by *Eco*RI and *Xho*I restriction digestion. For the reciprocal swap analysis, SPRYSEC-19 was cloned into pGADKT7 by using the restriction sites *Nde*I and *Bam*H1 from SPRYSEC-BD. Similarly, *Int-1/2-BD* was constructed by recloning *Int-1/2* from *Int-1/2-AD* into pGBKT7 from pACT-2 by using *Eco*R1 and *Xho*1 restriction sites.

In order to identify SPRYSEC-19 interactors, AH109 yeast cells were simultaneously co-transformed with pACT2 tomato cDNA library (prey) and bait (pGBKT7-SPRYSEC-19) according to the manufacturer's protocol. The transformants were plated on minimal SD agar base medium lacking four essential amino acids (–AHLW) but including X-α-gal followed by incubation at 30°C for 10 days. Blue colonies were selected as positive candidates followed by rescuing of AD plasmid following the manufacturer's instructions. The prey and bait plasmids did not autoactivate marker genes when co-transformed with empty bait and prey plasmids, respectively. For yeast mating, pGBKT7 constructs were introduced into yeast strain Y187 and AD plasmids (pACT2 and pGADKT7) were introduced into the AH109 yeast strain following the manufacturer's protocol. For each of Y187 and AH109 transformants, a 2- to 3-mm colony was vortexed in 200 µl of yeast peptone dextrose adenine and mixed together followed by incubation of the mixture at 30°C for 16 h with shaking. The transformants were spread on plates with minimal SD/–AHLW + X-α-gal medium followed by incubation at 30°C for 3 to 5 days.

Expression and purification of recombinant proteins from *Escherichia coli.*

The coding region of SPRYSEC-19 was PCR amplified from a *G. rostochiensis* cDNA library (Smant et al. 1998) using primers SpGF and SpGR with *Bam*H1 and *Xho*1 overhangs at the 5′ end and directionally cloned into pGEX-KG (Guan and Dixon 1991). For the THIO-LRR-SW5F construct, the LRR region of SW5F from the Int1/2-AD plasmid was isolated by restriction digestion (*Nco*1 and *Xho*1) and cloned into pET-32b (Novagen, Madison, WI, U.S.A.). The BL21 (DE3) cells were transformed with GST, GST-SPRYSEC-19, THIO, and THIO-LRR-SW5-F followed by induction with 1 mM isopropyl-β-D-thiogalactoside at 30°C for 5 h. The cells were lysed by sonication in 1× phosphate-buffered saline containing a complete protease inhibitor cocktail (Roche, Branchburg, NJ, U.S.A.) and the resulting supernatant was stored at –20°C until use.

In vitro GST pull-down assay.

The protocol for the GST pull-down assay was adopted from Nguyen and Goodrich (2006). The soluble fraction of bacterial lysate containing either GST or GST-SPRYSEC-19 was incubated with glutathione sepharose 4B beads (Amersham) for 2 h at 4°C followed by removal of lysate by centrifugation. To bound GST or GST-SPRYSEC-19, THIO-LRR-SW5-F or THIO alone were added and incubated at 4°C for 4 h. As negative control, sepharose beads were incubated with THIO and THIO-LRR-SW5-F.

Cloning of SW5-F.

To amplify full-length SW5F from tomato cv. GCR-161 (Kroon and Elgersma 1993), 100 mg of leaf tissue was ground in liquid nitrogen and total RNA was isolated using an Invisorb spin plant RNA minikit (Invitek, Berlin). First-strand cDNA was prepared from 5 µg of total RNA using Superscript first-strand cDNA synthesis kit (Invitrogen) following the manufacturer's protocol. The cDNA was used for amplification using a BD Advantage 2 PCR kit (BD Life Sciences, Boston) with primers SW5CD in combination with Int1/2-R. The amplification product of approximately 4 kb was cloned into pCR4 TOPO (Invitrogen) and sequenced.

ACKNOWLEDGMENTS

We are grateful for the valuable comments and suggestions made by J. T. Jones (SCRI) on the manuscript. S. Rehman, H. Overmars, and G. Smant were supported by an NWO Vernieuwingsimpuls grant. The work was further funded by the EU BIOEXPLOIT integrated project FOOD-CT-2005-513959. L. N. Spiridon and A.-J. Petrescu acknowledge support from the CNCSIS grant PN2-ID 168/2007.

LITERATURE CITED

Abad, P., Gouzy, J., Aury, J.-M., Castagnone-Sereno, P., Danchin, E. G. J., Deleury, E., Perfus-Barbeoch, L., Anthouard, V., Artiguenave, F., Blok, V. C., Caillaud, M.-C., Coutinho, P. M., Dasilva, C., De Luca, F., Deau, F., Esquibet, M., Flutre, T., Goldstone, J. V., Hamamouch, N., Hewezi, T., Jaillon, O., Jubin, C., Leonetti, P., Magliano, M., Maier, T. R., Markov, G. V., McVeigh, P., Pesole, G., Poulain, J., Robinson-Rechavi, M., Sallet, E., Segurens, B., Steinbach, D., Tytgat, T., Ugarte, E., van Ghelder, C., Veronico, P., Baum, T. J., Blaxter, M., Bleve-Zacheo, T., Davis, E. L., Ewbank, J. J., Favery, B., Grenier, E., Henrissat, B., Jones, J. T., Laudet, V., Maule, A. G., Quesneville, H., Rosso, M.-N., Schiex, T., Smant, G., Weissenbach, J., and Wincker, P. 2008. Genome sequence of the metazoan plant-parasitic nematode *Meloidogyne incognita*. Nat. Biotechnol. 26:909-915.

Bennett-Lovsey, R. M., Herbert, A. D., Sternberg, M. J. E., and Kelley, L. A. 2008. Exploring the extremes of sequence/structure space with ensemble fold recognition in the program Phyre. Proteins Struct. Funct. Genet. 70:611-625.

Blanchard, A., Esquibet, M., Fouville, D., and Grenier, E. 2005. Ranbpm homologue genes characterised in the cyst nematodes *Globodera pallida* and *Globodera 'mexicana'*. Physiol. Mol. Plant Pathol. 67:15-22.

Chenna, R., Sugawara, H., Koike, T., Lopez, R., Gibson, T. J., Higgins, D. G., and Thompson, J. D. 2003. Multiple sequence alignment with the Clustal series of programs. Nucleic Acids Res. 31:3497-3500.

Davis, E. L., Hussey, R. S., Mitchum, M. G., and Baum, T. J. 2008. Parasitism proteins in nematode–plant interactions. Curr. Opin. Plant. Biol. 11:1-7.

De Boer, J. M., Overmars, H. A., Bakker, J., and Gommers, F. J. 1992. Analysis of two-dimensional protein patterns from developmental stages of the potato cyst nematode, *Globodera rostochiensis*. Parasitology 105:461-474.

De Boer, J. M., Overmars, H. A., Pomp, H., Davis, E. L., Zilverentant, J. F., Goverse, A., Smant, G., Stokkermans, J. P. W. G., Hussey, R. S., Gommers, F. J., Bakker, J., and Schots, A. 1996. Production and characterization of monoclonal antibodies to antigens from second stage juveniles of the potato cyst nematode, *Globodera rostochiensis*. Fundam. Appl. Nematol. 19:545-545.

De Boer, J. M., Yan, Y., Smant, G., Davis, E. L., and Baum, T. J. 1998. In-situ hybridization to messenger RNA in *Heterodera glycines*. J. Nematol. 30:309-312.

De La Fuente Van Bentem, S., Vossen, J. H., De Vries, K. J., Van Wees, S., Tameling, W. I. L., Dekker, H. L., De Koster, C. G., Haring, M. A., Takken, F. L. W., and Cornelissen, B. J. C. 2005. Heat shock protein 90 and its co-chaperone protein phosphatase 5 interact with distinct regions of the tomato I-2 disease resistance protein. Plant J. 43:284-298.

Denti, S., Sirri, A., Cheli, A., Rogge, L., Innamorati, G., Putignano, S., Fabbri, M., Pardi, R., and Bianchi, E. 2004. RanBPM is a phosphoprotein that associates with the plasma membrane and interacts with the Integrin LFA-1. J. Biol. Chem. 279:13027-13034.

Fry, B. G., Vidal, N., Norman, J. A., Vonk, F. J., Scheib, H., Ramjan, S. F. R., Kuruppu, S., Fung, K., Hedges, S. B., Richardson, M. K., Hodgson, W. C., Ignjatovic, V., Summerhayes, R., and Kochva, E. 2006. Early evolution of the venom system in lizards and snakes. Nature 439:584-588.

Ghadessy, F. J., Chen, D., Kini, R. M., Chung, M. C. M., Jeyaseelan, K., Khoo, H. E., and Yuen, R. 1996. Stonustoxin is a novel lethal factor from stonefish (*Synanceja horrida*) venom. cDNA cloning and characterization. J. Biol. Chem. 271:25575-25581.

Grutter, C., Briand, C., Capitani, G., Mittl, P. R. E., Papin, S., Tschopp, J., and Grutter, M. G. 2006. Structure of the PRYSPRY-domain: Implica-

tions for autoinflammatory diseases. FEBS (Fed. Eur. Biol. Soc.) Lett. 580:99-106.
Guan, K., and Dixon, J. E. 1991. Eukaryotic proteins expressed in *Escherichia coli*: An improved thrombin cleavage and purification procedure of fusion proteins with glutathione S-transferase. Anal. Biochem. 192:262-267.
Hussey, R. S., and Grundler, F. M. W. 1998. Nematode parasitism of plants. Pages 213-243 in: Physiology and Biochemistry of Free Living and Plant Parasitic Nematodes. R. N. Perry and D. J. Wright, eds. CAB International, Oxon, U.K.
Jones, J. D. G., and Dangl, J. L. 2006. The plant immune system. Nature 444:323-329.
Junqueira-de-Azevedo, I. L. M., Ching, A. T. C., Carvalho, E., Faria, F., Nishiyama, M. Y., Jr., Ho, P. L., and Diniz, M. R. V. 2006. *Lachesis muta* (Viperidae) cDNAs reveal diverging pit viper molecules and scaffolds typical of cobra (Elapidae) venoms: Implications for snake toxin repertoire evolution. Genetics 173:877-889.
Kile, B. T., Schulman, B. A., Alexander, W. S., Nicola, N. A., Martin, H. M. E., and Hilton, D. J. 2002. The SOCS box: A tale of destruction and degradation. Trends Biochem. Sci. 27:235-241.
Kroon, B. A. M., and Elgersma, D. M. 1993. Interaction between race 2 of *Fusarium oxysporum* f. sp. *Lycopersici* and near-isogenic resistant and susceptible line of intact plants or callus of tomato. J. Phytopathol. 137:1-9.
Kudla, U., Milac, A. L., Qin, L., Overmars, H., Roze, E., Holterman, M., Petrescu, A. J., Goverse, A., Bakker, J., Helder, J., and Smant, G. 2007. Structural and functional characterization of a novel, host penetration-related pectate lyase from the potato cyst nematode *Globodera rostochiensis*. Mol. Plant Pathol. 8:293-305.
Li, S., Wang, J., Zhang, X., Ren, V., Wang, N., Zhao, K., Chen, X., Zhao, C., Li, X., Shao, J., Yin, J., West, M. B., Xu, N., and Liu, S. 2004. Proteomic characterization of two snake venoms: *Naja naja atra* and *Agkistrodon halys*. Biochem. J. 384:119-127.
Masters, S. L., Yao, S., Willson, T. A., Zhang, J. G., Palmer, K. R., Smith, B. J., Babon, J. J., Nicola, N. A., Norton, R. S., and Nicholson, S. E. 2006. The SPRY domain of SSB-2 adopts a novel fold that presents conserved Par-4-binding residues. Nat. Struct. Mol. Biol. 13:77-84.
Mucyn, T. S., Clemente, A., Andriotis, V. M. E., Balmuth, A. L., Oldroyd, G. E. D., Staskawicz, B. J., and Rathjen, J. P. 2006. The tomato NBARC-LRR protein Prf interacts with Pto kinase in vivo to regulate specific plant immunity. Plant Cell 18:2792-2806.
Murrin, L. C., and Talbot, J. N. 2007. RanBPM, a scaffolding protein in the immune and nervous systems. J. Neuro-Immunol. Pharm. 2:290-295.
Nakamura, M., Masuda, H., Horii, J., Kuma, K., Yokoyama, N., Ohba, T., Nishitani, H., Miyata, T., Tanaka, M., and Nishimoto, T. 1998. When overexpressed, a novel centrosomal protein, RanBPM, causes ectopic microtubule nucleation similar to gamma-tubulin. J. Cell Biol. 143:1041-1052.
Nguyen, T. N., and Goodrich, J. A. 2006. Protein-protein interaction assays: Eliminating false positive interactions. Nat. Methods 3:135-139.
Ponting, C., Schultz, J., and Bork, P. 1997. SPRY domains in ryanodine receptors (Ca2+-release channels). Trends Biochem. Sci. 22:193-194.
Pung, Y. F., Kumar, S. V., Rajagopalan, N., Fry, B. G., Kumar, P. P., and Kini, R. M. 2006. Ohanin, a novel protein from king cobra venom: Its cDNA and genomic organization. Gene 371:246-256.
Qin, L., Overmars, H., Helder, J., Popeijus, H., van der Voort, J. R., Groenink, W., van Koert, P., Schots, A., Bakker, J., and Smant, G. 2000. An efficient cDNA-AFLP-based strategy for the identification of putative pathogenicity factors from the potato cyst nematode *Globodera rostochiensis*. Mol. Plant-Microbe Interact. 13:830-836.
Rhodes, D. A., De Bono, B., and Trowsdale, J. 2005. Relationship between SPRY and B30.2 protein domains. Evolution of a component of immune defence. Immunology 116:411-417.
Sambrook, J., Fritsch, E. F., and Maniatis, T. 1989. Molecular Cloning: A Laboratory Manual. Cold Spring Harbor Laboratory Press, Cold Spring Harbor, NY, U.S.A.
Seto, M. H., Liu, H. L. C., Zajchowski, D. A., and Whitlow, M. 1999. Protein fold analysis of the B30.2-like domain. Proteins Struct. Funct. Genet. 35:235-249.
Smant, G., Goverse, A., Stokkermans, J., DeBoer, J. M., Pomp, H., Zilverentant, J. F., Overmars, H. A., Helder, J., Schots, A., and Bakker, J. 1997. Potato root diffusate-induced secretion of soluble, basic proteins originating from the subventral esophageal glands of potato cyst nematodes. Phytopathology 87:839-845.
Smant, G., Stokkermans, J., Yan, Y. T., de Boer, J. M., Baum, T. J., Wang, X. H., Hussey, R. S., Gommers, F. J., Henrissat, B., Davis, E. L., Helder, J., Schots, A., and Bakker, J. 1998. Endogenous cellulases in animals: Isolation of beta-1,4-endoglucanase genes from two species of plant-parasitic cyst nematodes. Proc. Natl. Acad. Sci. U.S.A. 95:4906-4911.
Spassova, M. I., Prins, T. W., Folkertsma, R. T., Klein-Lankhorst, R. M., Hille, J., Goldbach, R. W., and Prins, M. 2001. The tomato gene Sw5 is a member of the coiled coil, nucleotide binding, leucine-rich repeat class of plant resistance genes and confers resistance to TSWV in tobacco. Mol. Breed. 7:151-161.
Suyama, M., Torrents, D., and Bork, P. 2006. PAL2NAL: Robust conversion of protein sequence alignments into the corresponding codon alignments. Nucleic Acids Res. 34:W609-W612.
Ueda, A., Suzuki, M., Honma, T., Nagai, H., Nagashima, Y., and Shiomi, K. 2006. Purification, properties and cDNA cloning of neoverrucotoxin (neoVTX), a hemolytic lethal factor from the stonefish *Synanceia verrucosa* venom. Biochim. Biophys. Acta G 1760:1713-1722.
Van Ooijen, G., Burg Van Den, H. A., Cornelissen, B. J. C., and Takken, F. L. W. 2008a. Structure and function of resistance proteins in solanaceous plants. Annu. Rev. Phytopathol. 45:43-72.
Van Ooijen, G., Mayr, G., Kasiem, M. M., Albrecht, M., Cornelissen, B. J., and Takken, F. L. 2008b. Structure-function analysis of the NB-ARC domain of plant disease resistance proteins. J. Exp. Bot. 59:1383-1397.
Wang, D., Li, Z., Messing, E. M., and Wu, G. 2002. Activation of Ras/Erk pathway by a novel MET-interacting protein RanBPM. J. Biol. Chem. 277:36216-36222.
Wilson, I. A., and Stanfield, R. L. 1993. Antibody-antigen interactions. Curr. Opin. Struct. Biol. 3:113-118.
Woo, J. S., Imm, J. H., Min, C. K., Kim, K. J., Cha, S. S., and Oh, B. H. 2006. Structural and functional insights into the B30.2/SPRY domain. EMBO (Eur. Mol. Biol. Organ.) J. 25:1353-1363.
Xie, J., Sun, M., Guo, L., Liu, W., Jiang, J., Chen, X., Zhou, L., and Gu, J. 2006. Human Dectin-1 isoform E is a cytoplasmic protein and interacts with RanBPM. Biochem. Biophys. Res. Commun. 347:1067-1073.
Yang, Z. 2007. PAML 4: Phylogenetic analysis by maximum likelihood. Mol. Biol. Evol. 24:1586-1591.
Yang, Z., and Nielsen, R. 2000. Estimating synonymous and nonsynonymous substitution rates under realistic evolutionary models. Mol. Biol. Evol. 17:32-43.
Yuan, Y., Fu, C., Chen, H., Wang, X., Deng, W., and Huang, B. R. 2006. The Ran binding protein RanBPM interacts with TrkA receptor. Neurosci. Lett. 407:26-31.